A quadratic GFEM formulation for fracture mechanics problems

Murilo H.C. Bento[1], Caio S. Ramos[1], Sergio P.B. Proença[1], Carlos A. Duarte[2]

[1]*Department of Structural Engineering, São Carlos School of Engineering, University of São Paulo*
Av. Trabalhador São-Carlense 400, 13566-590, São Carlos - SP, Brasil
m.bento@usp.br, caio_silva@usp.br, persival@sc.usp.br
[2]*Department of Civil and Environmental Engineering, University of Illinois at Urbana-Champaign*
205 North Mathews Ave., 61801-2352, Urbana - IL, USA
caduarte@illinois.edu

Abstract. The Generalized Finite Element Method (GFEM) is a Galerkin approach that generates numerical approximations belonging to a space obtained by augmenting FEM spaces with enrichment functions capable of representing well local behaviors of the problem solution. The method has already proved to accurately solve different classes of problems, including those within the linear elastic fracture mechanics context. For these problems, GFEM shape functions can represent both the discontinuous and singular behaviors of cracks by a convenient choice of enrichment functions. Regarding convergence and conditioning aspects, recent works have proposed well-conditioned and optimally convergent first-order approximations based on GFEM enrichments. In this work, an initial version of a well-conditioned quadratic GFEM for problems of fracture mechanics is presented. The methodology consists of using a quadratic Partition of Unity (PoU) to combine local approximation spaces. A two-dimensional (2-D) numerical experiment with a linear elastic fracture mechanics problem is presented to demonstrate that the proposed formulation delivers optimal convergence and well-conditioned systems of equations. Moreover, the robustness of the proposed approach is also demonstrated by showing that the stiffness matrix conditioning is preserved even for some critical situations regarding the relative position between the mesh and the crack line.

Keywords: GFEM, Quadratic, Convergence, Conditioning.

1 Introduction

The Generalized Finite Element Method (GFEM), as in Duarte et al. [1] and Strouboulis et al. [2], has proved to effectively and accurately solve classes of problems that present challenging behaviors for standard methodologies, such as the Finite Element Method (FEM). One of the main features of the GFEM is that it can insert into its numerical approximations functions that can represent well some special local behaviors of the problem solution. As already reported extensively in the literature, problems within the Linear Elastic Fracture Mechanics (LEFM) can highly benefit from this feature. In particular, both the discontinuous and singular behaviors related to cracks can be added to the approximation using a proper choice of enrichment functions, which augment the standard FEM approximation space. Among other improvements, this fact largely alleviates some of the requirements related to mesh generation and regeneration, as in crack propagation problems, for instance, since the mesh no longer needs to fit the crack. In addition, reduced error levels and higher rates of convergence than the FEM can be attained when using the GFEM.

As reported by Zhang et al. [3] and Babuška et al. [4], three features are important to develop a stable GFEM formulation: optimal convergence, stiffness matrix conditioning similar to the FEM formulation, and robust conditioning. This last feature guarantees that the conditioning does not depend on relative positions between the mesh and the crack line for problems within the LEFM, for instance. Recent works have already shown the good capacity of the GFEM to deliver optimal first-order convergent solutions with well-behaved and robust conditioning, as in Sanchez-Rivadeneira and Duarte [5] and Cui and Zhang [6]. In particular, the work of Sanchez-Rivadeneira and Duarte [5] developed a simple approximation using shifted Heaviside functions and the discontinuous sta-

ble GFEM (DSGFEM), see Sanchez-Rivadeneira and Duarte [7], for the branch functions. Moreover, in Cui and Zhang [6], based on the work of Zhang et al. [8], different Partitions of Unity (PoUs) and other techniques are used to control the stiffness matrix conditioning.

Laborde et al. [9] can be considered as one of the first works dedicated to the development of higher-order convergent approximations for problems within the LEFM context. The methodology adopted by the authors introduced the use of quadratic PoUs to reach higher-order convergence, but the final approximation led to sub-optimal convergence or badly-conditioned stiffness matrices. This was due to its choice of enrichment functions. More recent works still focus on finding a good enriched space that delivers higher-order convergence, such as in Sanchez-Rivadeneira and Duarte [7] and Sanchez-Rivadeneira et al. [10] for fracture mechanics problems, and in Zhang and Babuška [11] for interface problems. However, to the best of our knowledge, alternatives for higher-order approximations are still under investigation. Therefore, a quadratic formulation based on the use of quadratic PoUs, similar to one of the strategies proposed by Sanchez-Rivadeneira and Duarte [7], is investigated herein. Based on some numerical experiments, it is shown that the formulation presents the required features to be considered stable.

Following this introduction, Section 2 presents the weak formulation of the LEFM problem which is investigated throughout this work. Section 3 details the quadratic GFEM used to approximately solve that class of problem. Then, Section 4 illustrates the two-dimensional (2-D) numerical experiment conceived, as well as the main results and discussions. Finally, Section 5 summarizes the main conclusions.

2 Fracture mechanics problem

In this section, the LEFM problem to be investigated is defined. Consider a body $\bar{\Omega} \subset \mathbb{R}^2$, with boundary $\partial\Omega$ in which a traction $\bar{\boldsymbol{t}}$ is applied. This is a Neumann boundary value problem. It is assumed that the body contains a crack Γ_c, considered herein as traction-free. The variational, or weak, formulation for this class of problems can be given by:

Find $\boldsymbol{u} \in \mathcal{E}(\Omega)$ such as, for all $\boldsymbol{v} \in \mathcal{E}(\Omega)$,

$$B(\boldsymbol{u}, \boldsymbol{v}) = L(\boldsymbol{v}), \tag{1}$$

with

$$B(\boldsymbol{u}, \boldsymbol{v}) = \int_\Omega \boldsymbol{\sigma}(\boldsymbol{u}) \colon \boldsymbol{\varepsilon}(\boldsymbol{v}) \, \mathrm{d}S \quad \text{and} \quad L(\boldsymbol{v}) = \int_{\partial\Omega} \bar{\boldsymbol{t}} \cdot \boldsymbol{v} \, \mathrm{d}s. \tag{2}$$

For more details regarding this formulation, see the work of Szabo and Babuška [12]. The space $\mathcal{E}(\Omega) \subset (H^1(\Omega))^2$ is the well-known energy space, in which the following energy norm can be defined:

$$\|\boldsymbol{u}\|_{\mathcal{E}(\Omega)} = \sqrt{B(\boldsymbol{u}, \boldsymbol{u})} < \infty. \tag{3}$$

3 Quadratic GFEM

The GFEM is a Galerkin approach that generates numerical approximations belonging to a space obtained by augmenting a standard FEM space $\mathcal{S}_{\mathrm{FEM}}$ with functions capable to represent well local behaviors of the problem solution. These functions are known as enrichment functions and, combined with a Partition of Unity, are used to generate the enriched space $\mathcal{S}_{\mathrm{ENR}}$. Therefore,

$$\mathcal{S}_{\mathrm{GFEM}} = \mathcal{S}_{\mathrm{FEM}} + \mathcal{S}_{\mathrm{ENR}}. \tag{4}$$

The objective herein is to generate a quadratic approximation $\hat{\boldsymbol{u}} \in \mathcal{S}_{\mathrm{GFEM}}$, therefore delivering a convergence rate of relative errors in the energy norm, with respect to the finite element size, equals to 2.

Thus, to span the $\mathcal{S}_{\mathrm{FEM}}$ space a quadratic basis is herein adopted, i.e.,

$$\mathcal{S}_{\mathrm{FEM}} = \sum_{\alpha=1}^{n} \boldsymbol{u}_\alpha \, \psi_\alpha(\boldsymbol{x}), \quad \text{with} \quad \boldsymbol{u}_\alpha \in \mathbb{R}^2 \tag{5}$$

and $\psi_\alpha(\boldsymbol{x})$ a quadratic PoU. Herein, this PoU is the set of conventional FEM shape functions that has the Kronecker's delta property and it is attached to 6-node triangular finite elements. In Eq. (5), n represents the total number of nodes that accounts for both vertex and edge nodes.

3.1 Enriched space for LEFM

The enriched space $\mathcal{S}_{\mathrm{ENR}}$ in the LEFM context must be able to represent the following behaviors: the crack discontinuity and the crack tip singularity. This enriched space can, thus, be accordingly split into two subspaces: $\mathcal{S}^D_{\mathrm{ENR}}$ and $\mathcal{S}^S_{\mathrm{ENR}}$.

First, the space $\mathcal{S}^D_{\mathrm{ENR}}$ is devoted to representing the crack discontinuity and it is, in this work, generated using shifted Heaviside enrichment functions, i.e.,

$$\mathcal{S}^D_{\mathrm{ENR}} = \sum_{\alpha \in \mathscr{I}_1} \psi_\alpha(\boldsymbol{x}) \left(\mathcal{H}(\boldsymbol{x}) - \mathcal{H}(\boldsymbol{x}_\alpha)\right) \boldsymbol{u}^D_\alpha, \quad \text{with} \quad \boldsymbol{u}^D_\alpha \in \mathbb{R}^2 \tag{6}$$

and $\mathcal{H}(\boldsymbol{x})$ representing the Heaviside function. This function is defined as follows: 1, if $\Gamma_c \geq 0$, or -1 otherwise. This enrichment function is applied at the set of nodes whose indexes are in $\mathscr{I}_1$, an index set given by:

$$\mathscr{I}_1 = \{\alpha \in \mathscr{I} : \, \omega_\alpha \cap \Gamma_c \neq \emptyset \text{ and } C \notin \omega_\alpha\}. \tag{7}$$

with $\mathscr{I}$ representing the index set of all mesh nodes, including both vertex and edge nodes, and C the crack tip. In addition, ω_α represents the cloud of node $\boldsymbol{x}_\alpha$, which is given by the union of all the elements sharing this node.

On the other hand, the space $\mathcal{S}^S_{\mathrm{ENR}}$ is used to represent the crack tip singularity and it is generated, in this work, based on the OD vector-valued branch functions, i.e.,

$$\mathcal{S}^S_{\mathrm{ENR}} = \sum_{\alpha \in \mathscr{I}_2} \psi_\alpha(\boldsymbol{x}) \sum_{i=1}^{2} \left(\mathcal{L}^S_{\alpha i}(\boldsymbol{x}) - \mathcal{D}_{\omega_\alpha}[\mathcal{L}^S_{\alpha i}](\boldsymbol{x})\right) \odot \boldsymbol{u}^S_{\alpha i}, \quad \text{with} \quad \boldsymbol{u}^S_{\alpha i} \in \mathbb{R}^2 \tag{8}$$

and $\mathcal{L}^S_{\alpha i}(\boldsymbol{x})$ the OD branch functions. These functions represent the displacement behavior near the crack tip for both opening Modes I and II, given by:

$$\mathcal{L}^{\mathrm{S}}_{\alpha 1} = \left[\sqrt{r}\cos\frac{\theta}{2}\left(\kappa - 1 + 2\sin^2\frac{\theta}{2}\right), \; \sqrt{r}\sin\frac{\theta}{2}\left(\kappa + 1 + 2\cos^2\frac{\theta}{2}\right)\right]^{\mathrm{T}} \tag{9}$$

$$\mathcal{L}^{\mathrm{S}}_{\alpha 2} = \left[\sqrt{r}\sin\frac{\theta}{2}\left(\kappa + 1 - 2\cos^2\frac{\theta}{2}\right), \; -\sqrt{r}\cos\frac{\theta}{2}\left(\kappa - 1 - 2\sin^2\frac{\theta}{2}\right)\right]^{\mathrm{T}}, \tag{10}$$

In the previous equations, (r, θ) corresponds to a local polar coordinate system attached to the crack tip (see Fig. 1, next) and κ represents a material constant given by $\kappa = 3 - 4\nu$ for plane strain and $\kappa = (3-\nu)/(1+\nu)$ for plane stress conditions. The functions $\mathcal{L}^{\mathrm{S}}_{\alpha i}$ are assigned to the set of nodes whose indexes are in $\mathscr{I}_2$, an index set given by:

$$\mathscr{I}_2 = \{\alpha \in \mathscr{I} : \ \mathrm{dist}(C, \boldsymbol{x}_\alpha) < r_{\mathrm{br}}\}, \tag{11}$$

with r_{br} a discretization parameter.

In the expressions given by Eqs. (6) and (8), two strategies were already adopted to keep the stiffness matrix conditioning under control, namely the Heaviside shifting and the subtraction from the OD branch functions of their discontinuous interpolant. For a comprehensive explanation on how to compute this interpolant and implement it, see the work of Sanchez-Rivadeneira and Duarte [7].

Remark 1: Stiffness matrix conditioning. It is well known that the conditioning of GFEM stiffness matrices can be much worse than that of FEM matrices. This is caused when the adopted enrichment functions cause linear or nearly-linear dependencies between the set of shape functions. The work of Babuška and Banerjee [13] presents a detailed explanation related to this topic. Here, the stiffness matrix conditioning is measured using its Scaled Condition Number (SCN). The SCN $\mathcal{K}(\boldsymbol{K})$ can be computed as the ratio between the largest (λ_M) and smallest non-zero (λ_m) eigenvalues of the scaled matrix $\hat{\boldsymbol{K}}$, i.e.,

$$\mathcal{K}(\boldsymbol{K}) = \frac{\lambda_M}{\lambda_m}.$$

with $\hat{K}_{ij} = K_{ij}/\sqrt{K_{ii}\,K_{jj}}$, and no summation on i, j. Herein, since pure Neumann problems are being analyzed, the three first null eigenvalues are not accounted for because they are solely related to rigid body motions.

The corresponding numerical approximation generated by the space given by Eq. (4) can be understood as an extension of the formulation proposed initially by Sanchez-Rivadeneira and Duarte [5], using now quadratic PoUs to attain quadratic convergence rates. The approximation adopted herein is similar to what is presented in Sanchez-Rivadeneira and Duarte [7] with strategy ES-B. However, a different set of numerical tests is performed in the present work. They demonstrate, for the first time, the robustness of this quadratic approximation.

4 Numerical tests

4.1 Problem description

In this section, a two-dimensional LEFM problem is solved to illustrate the new quadratic GFEM. This pure Neumann problem consists of a square panel $\bar{\Omega} = [0, 1] \times [0, 1]$ containing a horizontal edge-crack Γ_c given by:

$$\Gamma_c = \{(x_1, x_2) \in \mathbb{R}^2 \colon 0 \leq x_1 \leq 1/2 \ \text{ and } \ x_2 = 1/2 + \delta\}, \tag{12}$$

with $\delta = 0$ unless stated otherwise. The problem geometry and Neumann boundary conditions, as well as the crack Γ_c, are illustrated in Fig. 1.

As material properties, an Young's modulus $E = 1$ and a Poisson's ratio $\nu = 0.3$ are adopted, and plane strain conditions are assumed. The traction applied at $\partial\Omega$ is computed from the first term of the asymptotic expansion that is the solution of an infinite plate subjected to Mode I traction containing a horizontal crack, given by:

$$\sigma^{\mathrm{I}}_{11} = \frac{1}{4\sqrt{r}}\left(3\cos\frac{\theta}{2} + \cos\frac{5\theta}{2}\right) \tag{13}$$

$$\sigma^{\mathrm{I}}_{22} = \frac{1}{4\sqrt{r}}\left(5\cos\frac{\theta}{2} - \cos\frac{5\theta}{2}\right) \tag{14}$$

$$\sigma^{\mathrm{I}}_{12} = \frac{1}{4\sqrt{r}}\left(-\sin\frac{\theta}{2} + \sin\frac{5\theta}{2}\right), \tag{15}$$

with (r, θ) the polar coordinate system attached to the crack tip, as illustrated in Fig. 1 (left).

The problem is discretized using quadratic triangular finite elements, as shown in Fig. 1 (right). The mesh is generated by subdividing each side of the panel by the following numbers of subdivisions:

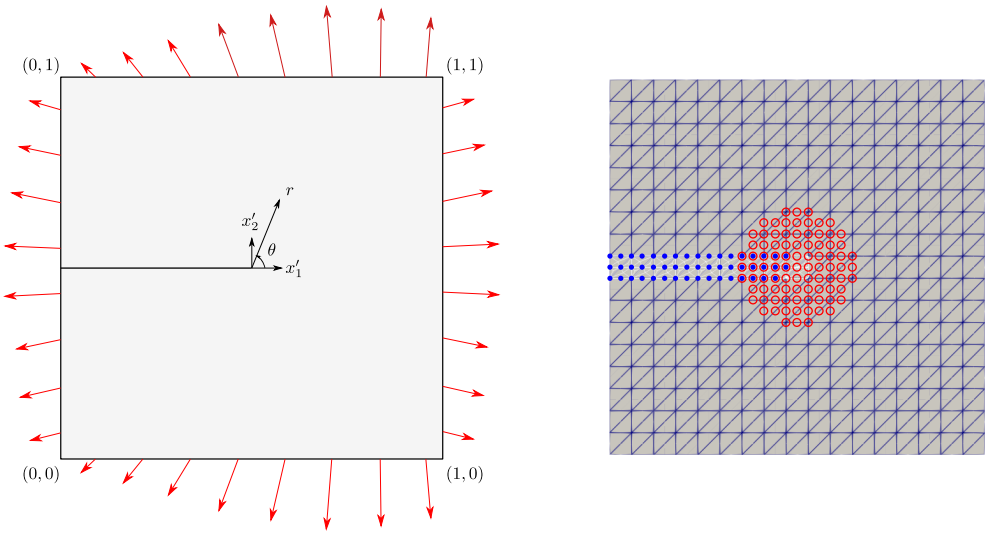

Figure 1. Problem geometry and Neumann boundary conditions (left), and the less refined adopted discretization, with $N_{\text{div}} = 17$, (right) for the numerical problem. In the right figure, the blue dots represent the nodes enriched with Heaviside functions and the red ones the nodes enriched with OD branch functions.

$$N_{\text{div}} = 2^{j+3} + 1, \quad \text{with} \quad j = 1, 2, 3, 4, 5. \tag{16}$$

Once defined the number of subdivisions, a structured mesh of 6-node triangular elements can be constructed. Finally, to define the regions where the enrichment functions are applied, the parameters $C = (1/2, 1/2 + \delta)$ and $r_{\text{br}} = 1/6$ are adopted in Eqs. (7) and (11).

4.2 Results and discussions

First, the convergence of relative errors in the energy norm is evaluated. As already highlighted in Section 3, a rate of convergence $\mathcal{O}(h^2)$ is expected for the quadratic formulation presented in this work. The relative error in the energy norm is computed using

$$\epsilon_h = \frac{\|\boldsymbol{u} - \hat{\boldsymbol{u}}\|_{\mathcal{E}(\Omega)}}{\|\boldsymbol{u}\|_{\mathcal{E}(\Omega)}} = \frac{\sqrt{\int_\Omega (\boldsymbol{\sigma}(\boldsymbol{u}) - \boldsymbol{\sigma}(\hat{\boldsymbol{u}})) : (\boldsymbol{\varepsilon}(\boldsymbol{u}) - \boldsymbol{\varepsilon}(\hat{\boldsymbol{u}}))\, \mathrm{d}S}}{\sqrt{\int_\Omega \boldsymbol{\sigma}(\boldsymbol{u}) : \boldsymbol{\varepsilon}(\boldsymbol{u})\, \mathrm{d}S}}, \tag{17}$$

with $\boldsymbol{u}$ the problem exact displacement solution, known from the LEFM.

The plot presented in Fig. 2 (left) illustrates the convergence of relative errors ϵ_h with respect to the finite element size $h^{-1} = N_{\text{div}}$. In the plot, the dashed gray line represents the optimal rate $\beta = 2$. It can be seen that the convergence rate tends to this optimal value as the mesh is refined, i.e., as $h \to 0$.

In addition, as also specified in Section 3, the growth rate of the stiffness matrix SCN $\mathcal{K}(\boldsymbol{K})$ is another important quantity to be evaluated when assessing the new GFEM formulation. According to the works of Zhang et al. [3] and Babuška et al. [4], the conditioning growth rate should not be greater than the one obtained when using the standard FEM, which is $\mathcal{O}(h^{-2})$ for 2-D Neumann problems. For that matter, Fig. 2 (right) illustrates the SCN values for each one of the adopted approximations. Again, the dashed gray line represents the optimal rate $\beta = 2$. It is important to say that controlled values of $\mathcal{K}(\boldsymbol{K})$ help to eliminate possible round-off errors and convergence issues when solving the problem system of equations either directly or iteratively.

Finally, seeking at evaluating the robustness of the stiffness matrix conditioning, the following experiment is performed: the crack is moved from its initial position, i.e., when $\delta = 0$, up to the finite element edges, with the

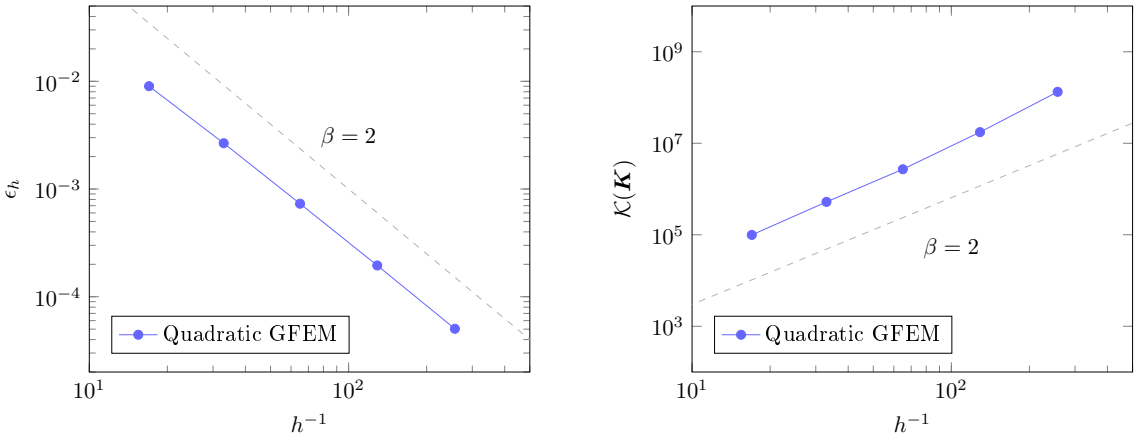

Figure 2. Convergence of relative errors in the energy norm (left) and growth of the stiffness matrix SCN (right) with respect to the finite element size.

parameter δ in Eq. (12) computed as

$$\delta = h \times (1 - 2^j) \,/\, 2,$$

with $j = 0, -2, \ldots, -10$. It can be noticed that if $j = 0$, the crack cuts through the middle of finite element edges in the x_2 direction, and as j decreases the crack moves up to the finite element edges in the x_1 direction, with $\delta \to h/2$ when $j \to -\infty$.

To perform these analyses, the mesh obtained with the first level of refinement, i.e., $N_{\text{div}} = 17$, is adopted. The blue curve in Fig. 3 illustrates the SCN $\mathcal{K}(\boldsymbol{K})$ for each value of δ. It is observed that, when the crack is very close to finite element edges, the SCN starts to increase. In the present work, a node snapping (NS) strategy is adopted to control this behavior. Herein, the algorithm presented by Sanchez-Rivadeneira and Duarte [7], that moves the nodes that are very close to the crack towards its line, is applied.

The nodes moved are the ones in which

$$\delta_\alpha^{\text{closest}} \,/\, h_\alpha^{\max} < \delta^{\text{snap}},$$

with $\delta_\alpha^{\text{closest}}$ the closest distance between the node and the crack, and $h_\alpha^{\max}$ the biggest distance between the node and its vertex neighbors. Herein, it is adopted $\delta^{\text{snap}} = 5\%$. It is important to highlight that this node snapping strategy is only applied at vertex nodes. The edge nodes are only moved in order to keep them in the middle of their corresponding edges.

Applying this NS strategy, the conditioning is again controlled. This can be seen in the green plot of Fig. 3.

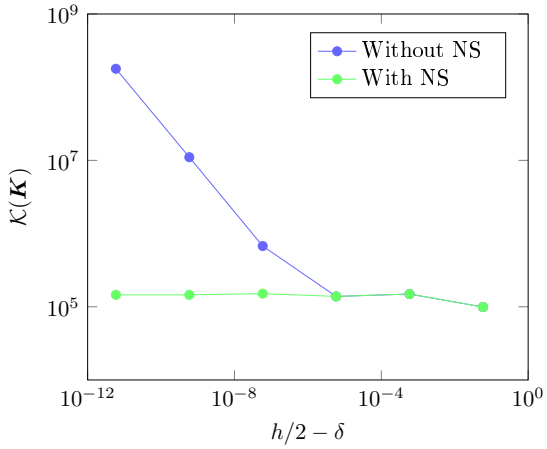

Figure 3. Robustness test for the numerical problem and $N_{\text{div}} = 17$.

5 Conclusions

This work aims at developing a simple and accurate quadratic GFEM formulation based on the quadratic Partitions of Unity (PoUs) usually adopted as shape functions within the standard FEM context. The approximation proposed in this paper can be understood as an extension of the work of Sanchez-Rivadeneira and Duarte [5], since the same enrichment functions are herein adopted, and it is closely related to strategy ES-B presented by Sanchez-Rivadeneira and Duarte [7]. The GFEM formulation delivered, for the investigated numerical problem of Section 4.1, quadratic convergence in the energy norm and well-conditioned stiffness matrices, with a SCN growth rate not greater than what is reached by the FEM. Herein, other situations regarding the relative position between the crack and the finite element mesh are investigated to assess the robustness of the method. The robustness of the proposed approach is also demonstrated by showing that the stiffness matrix conditioning is preserved even for critical situations regarding the relative position between the mesh and the crack line.

Acknowledgments. The first three authors would like to acknowledge the support provided by the University of São Paulo (USP) and the financial support provided by the São Paulo Research Foundation (FAPESP) under process numbers 2019/00435-3 and 2020/14463-6. C.A. Duarte would like to acknowledge the support from the University of Illinois at Urbana-Champaign (UIUC).

Authorship statement. The authors hereby confirm that they are the sole liable persons responsible for the authorship of this work, and that all material that has been herein included as part of the present paper is either the property (and authorship) of the authors, or has the permission of the owners to be included here.

References

[1] C. Duarte, I. Babuška, and J. Oden. Generalized finite element methods for three-dimensional structural mechanics problems. *Computers & Structures*, vol. 77, pp. 215–232, 2000.
[2] T. Strouboulis, K. Copps, and I. Babuška. The generalized finite element method. *Computer Methods in Applied Mechanics and Engineering*, vol. 190, pp. 4081–4193, 2001.
[3] Q. Zhang, I. Babuška, and U. Banerjee. Robustness in stable generalized finite element methods (SGFEM) applied to Poisson problems with crack singularities. *Computer Methods in Applied Mechanics and Engineering*, vol. 311, pp. 476–502, 2016.
[4] I. Babuška, U. Banerjee, and K. Kergrene. Strongly stable generalized finite element method: Application to interface problems. *Computer Methods in Applied Mechanics and Engineering*, vol. 327, pp. 58–92, 2017.
[5] A. Sanchez-Rivadeneira and C. Duarte. A simple, first-order, well-conditioned, and optimally convergent Generalized/eXtended FEM for two- and three-dimensional linear elastic fracture mechanics. *Computer Methods in Applied Mechanics and Engineering*, vol. 372, pp. 113388, 2020.
[6] C. Cui and Q. Zhang. Stable generalized finite element method for elasticity crack problems. *International Journal for Numerical Methods in Engineering*, vol. 121, pp. 3066–3082, 2020.
[7] A. Sanchez-Rivadeneira and C. Duarte. A stable generalized/eXtended FEM with discontinuous interpolants for fracture mechanics. *Computer Methods in Applied Mechanics and Engineering*, vol. 345, pp. 876–918, 2019.
[8] Q. Zhang, U. Banerjee, and I. Babuška. Higher order stable generalized finite element method. *Numerische Mathematik*, vol. 128, pp. 1–29, 2014.
[9] P. Laborde, J. Pommier, Y. Renard, and M. Salaun. High-order extended finite element method for cracked domains. *International Journal for Numerical Methods in Engineering*, vol. 64, pp. 354–381, 2005.
[10] A. Sanchez-Rivadeneira, N. Shauer, B. Mazurowski, and C. Duarte. A Stable Generalized/eXtended p-hierarchical FEM for three-dimensional linear elastic fracture mechanics. *Computer Methods in Applied Mechanics and Engineering*, vol. 364, pp. 112970, 2020.
[11] Q. Zhang and I. Babuška. A stable generalized finite element method (SGFEM) of degree two for interface problems. *Computer Methods in Applied Mechanics and Engineering*, vol. 363, pp. 112889, 2020.
[12] B. Szabo and I. Babuška. *Finite Element Analysis*. John Wiley and Sons, New York, 1991.
[13] I. Babuška and U. Banerjee. Stable Generalized Finite Element Method (SGFEM). *Computer Methods in Applied Mechanics and Engineering*, vol. 201–204, pp. 91–111, 2012.